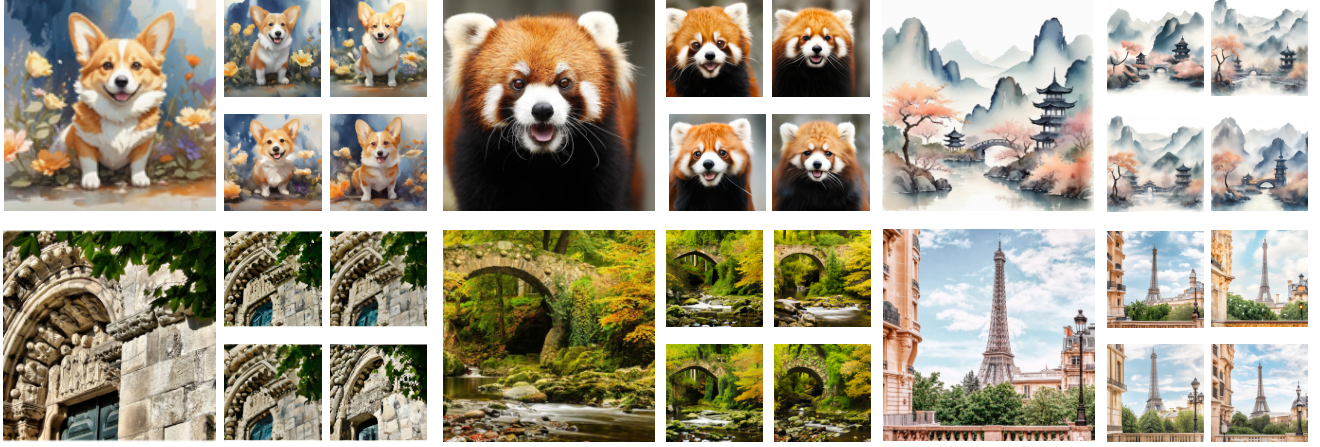


# Visual Lexicon: Rich Image Features in Language Space

XuDong Wang<sup>1,2\*</sup> Xingyi Zhou<sup>1</sup> Alireza Fathi<sup>1</sup> Trevor Darrell<sup>2</sup> Cordelia Schmid<sup>1</sup>  
<sup>1</sup>Google DeepMind <sup>2</sup>UC Berkeley



**Figure 1.** Given the cute corgi painting in the top left corner, how can we extract a visual representation that captures semantic-level information – such as object categories and layouts – while preserving rich visual details like image styles, textures and colors? **We introduce ViLex model that generates image representations in the text vocabulary space**, acting as a new visual “language”, while retaining intricate visual details that are difficult, if not impossible, to convey in natural language. The set of images (generated under different diffusion noises) in the 2×2 grid, which are highly semantically and visually similar to each other, is created by using ViLex as “text” prompts for text-to-image diffusion models.

## Abstract

We present *Visual Lexicon*, a novel visual language that encodes rich image information into the text space of vocabulary tokens while retaining intricate visual details that are often challenging to convey in natural language. Unlike traditional methods that prioritize either high-level semantics (e.g., CLIP) or pixel-level reconstruction (e.g., VAE), ViLex simultaneously captures rich semantic content and fine visual details, enabling high-quality image generation and comprehensive visual scene understanding. Through a self-supervised learning pipeline, ViLex generates tokens optimized for reconstructing input images using a frozen text-to-image (T2I) diffusion model, preserving the detailed information necessary for high-fidelity semantic-level reconstruction. As an image embedding in the language space, ViLex tokens leverage the compositionality of natural languages, allowing them to be used independently as “text tokens” or combined with natural language tokens to prompt

pretrained T2I models with both visual and textual inputs, mirroring how we interact with vision-language models (VLMs). Experiments demonstrate that ViLex achieves higher fidelity in image reconstruction compared to text embeddings—even with a single ViLex token. Moreover, ViLex successfully performs various DreamBooth tasks in a zero-shot, unsupervised manner without fine-tuning T2I models. Additionally, ViLex serves as a powerful vision encoder, consistently improving vision-language model performance across 15 benchmarks relative to a strong SigLIP baseline.

## 1. Introduction

How should we represent an image? This is a fundamental question in computer vision. Over decades of progress, there have been two primary approaches: representations optimized for understanding high-level semantics [14, 50, 53], or for high-fidelity image reconstruction [23, 34, 86], often used in image generation [55, 60]. Understanding-focused models like CLIP [53] and DINO [8] capture high-level semantics but lose pixel-level details. Conversely,

\*Work done in a Google DeepMind internship.  
 ✉{xudongwang, zhouxy}@google.com

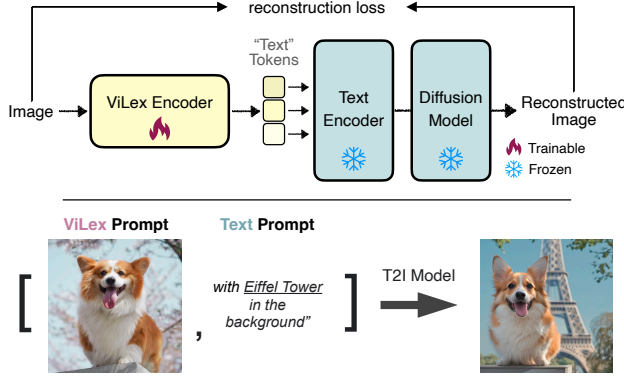


**Figure 2. top) ViLex empowers linguistic space to capture visual richness.** We propose ViLex, an image encoder that maps images into the vocabulary space, effectively preserving semantic information and intricate visual details. The embeddings from ViLex function as a *Visual Lexicon* that preserve semantic and intricate visual details of the image. ViLex is trained with a frozen text-to-image diffusion model and can be utilized independently as “text” tokens for image generation. **bottom) Linguistic space empowers ViLex to enjoy compositionality.** ViLex can be combined with natural language tokens for prompting a pretrained T2I diffusion models with both visual and textual cues.

reconstruction-focused models, such as VAEs [34], retain fine visual details but lack semantic richness, making them less effective for tasks like vision-language modeling. In this paper, we aim to address the question: “*can a single representation excel in both image reconstruction and semantic understanding?*”

To bridge this gap, we introduce ViLex that encodes images into a **Visual Lexicon** within the text space. ViLex model is designed to capture both high-level semantics – such as object categories and spatial layouts – while preserving rich visual details like styles, and textures that are difficult or even impossible to articulate in natural language.

We achieve this, as illustrated in Figure 2, by leveraging a self-supervised learning strategy based on a frozen, pretrained text-to-image (T2I) diffusion model, which acts as the source of supervisory signals. Although initially developed for generative purposes, many recent works [3, 19, 35, 79] have discovered that diffusion models [27, 56, 60] inherently capture both semantic and detailed visual information through their denoising process.

To incorporate rich visual information into our ViLex model, we repurpose diffusion models as decoders within an autoencoder [4, 25, 34, 73] framework. ViLex embeddings are mapped into the latent space of the T2I diffusion model’s vocabulary tokens—specifically, the index-to-embedding lookup matrix of the text encoder [53, 54], which converts text token IDs into embeddings. Using diffusion models as decoders for *semantic-level image reconstruction*, rather than traditional VAE decoders [34] or

MAE [23] designed for *pixel-level reconstruction*, encourages the model to learn meaningful semantic representations that are highly transferable to diverse visual scene understanding tasks. This design enables ViLex to harness the rich visual knowledge embedded in diffusion models while maintaining a lightweight structure, making it well-suited for a broad range of understanding tasks beyond diffusion models’ original generative applications.

The ViLex model consists of a vision encoder that extracts visual representations from the input image and an attention pooling layer that transforms the visual representation into visual lexicon tokens. During training, ViLex model is optimized with an image reconstruction loss, receiving gradients from the frozen diffusion model and its text encoder to fine-tune the visual lexicon tokens for accurately reconstructing images with similar appearance. Additionally, we propose the TailDrop strategy during training, where the last  $k$  visual lexicon tokens are randomly dropped to encourage the earlier tokens to encapsulate richer semantic information. During inference, the number of tokens can be dynamically adjusted to meet user requirements.

Our ViLex model is designed to support both image generation and understanding tasks. **For image generation:** ViLex tokens can be directly used as “text-prompts”, enabling the re-creation of semantically and visually similar images. Experiments on COCO image reconstruction demonstrate that our ViLex significantly outperforms its counterparts image-guided DALL-E 3 [5] and DeDiffusion [76] in terms of the layout, semantic, and style consistency with the input image, based on human studies. Notably, even with just a single ViLex token, the FID score of ViLex remains lower than that of DeDiffusion [76], showcasing the representational power of Visual Lexicon. Additionally, ViLex embeddings can seamlessly integrate with text prompts, for example, “*an image similar to [ViLex tokens], in Van Gogh style*”, enabling **multimodal image generation** and DreamBooth [58] tasks in a zero-shot fashion by prompting a frozen T2I model with both visual and textual inputs. **For image understanding:** replacing the strong semantic-pretrained backbone SigLIP [88] with ViLex’s vision encoder in vision-language models [6] leads to improvements across various vision-language tasks, including image and video captioning [10, 78], visual question answering [21], and referring segmentation [83].

#### The main contributions of our work are:

- We propose ViLex, an image encoder that maps images into the text space of text-to-image diffusion models. The resulting image embeddings capture both high-level semantics and intricate visual details that are otherwise challenging to convey in natural language.
- ViLex enables zero-shot unsupervised DreamBooth by prompting T2I models with both ViLex tokens and text prompts, without requiring fine-tuning a T2I model or



modifying its architectures. ViLex also improves image reconstruction quality compared to previous baselines for generating semantically similar images, reducing FID by a large margin on MS-COCO using the same token count.

- ViLex enhances the understanding capability of the image embeddings. Replacing the image encoder in vision-language models with ViLex yields improved performance on various visual understanding tasks, including image/video captioning, visual question answering, and image referring segmentation.

## 2. Related Work

**Image Representation Learning** is a fundamental task in computer vision. There are two popular approaches: representing an image with features optimized for visual scene understanding [14, 20, 37, 50, 53, 72, 75, 77, 88] or with features optimized for high-fidelity image reconstruction [23, 34, 51, 86], which is often used in image generation [52, 60]. Understanding-focused representations like those in CLIP [53], SigLIP [88], DINO [8], and DINOv2 [8, 50] capture high-level semantic information but lose pixel-level details. Conversely, reconstruction-focused features, commonly from AutoEncoder-based models (AEs), like VAE [34], MAE [23], and BEiT [2], retain fine image details but often lack semantic richness, limiting their utility in downstream tasks like vision-language modeling [6, 36]. AutoEncoders, while effective for pixel-level fidelity, often struggle with discriminative tasks. Their focus on reconstructing local, semantically agnostic details leads to suboptimal performance in tasks demanding rich, discriminative representations, such as linear evaluation on ImageNet [2, 9, 15]. We intend to propose a new vision encoder that provides image representations for both image understanding and generation tasks.

**Image Inversion for Diffusion Models.** The goal of image inversion is to determine the text prompt that can be used for generating a specific source image. Prompt-inversion [44, 48] uses gradient descent to move from the pixel space to the text-embedding space. Techniques like Dreambooth [58, 59] and textual-inversion [18] learn special text tokens for given instances, but require gradient-based training for each individual image, making them slow at inference time. Also, DreamBooth needs to determine the LORA adapters for model architecture changes and is not generic for visual understanding. Recently, DeDiffusion [76] proposed training a model to generate the inverse text using Gumbel softmax, but the quality of reconstruction is limited by what can be represented by text tokens. Our approach bypasses discrete language-based text representations, enabling higher-quality reconstructions and efficient single-pass inference.

**Representation Learning with Diffusion Models** has been explored by several previous works [12, 31, 74, 79,

80, 84]. For instance, I-DAE [12] uses the diffusion loss as a self-supervised learning objective, while ODISE [79] employs diffusion-pretrained features for zero-shot panoptic segmentation. DIVA [74] shows that finetuning a CLIP backbone [53] with gradients from diffusion models enhances localization capabilities. In contrast to these methods, we harness the built-in knowledge of T2I models to learn visual features, effectively framing the generation of text embeddings that reconstruct an image as a powerful representation learning objective.

**Image Tokenization**, commonly associated with variational autoencoders (VAEs) [34], is crucial for compressing images into a lower-dimensional space for diffusion model training. VQVAEs [56, 81] utilizes a discrete codebook for quantizing latent representations, while recent works like MagViTv2 [85], FSQ [47], and BSQ [89] improve quantization with direct binary encoding. More recent image tokenizers [38, 71, 86] propose new encoding strategies, including scale prediction [38, 71] and 1D compression [86]. Unlike these tokenizers, which predict features as noise, our model predicts features conditioned on the diffusion model. Thus, instead of aiming for lossless reconstruction, our focus is on recreating images with high semantic fidelity.

## 3. Describe an Image with a Visual Lexicon

In this section, we introduce ViLex that maps images directly into the text space, while effectively preserving complex visual details that are difficult to express in natural language. Our representation effectively acts as a new “language” for text-to-image generation and a strong vision encoder for downstream vision-language tasks. We will introduce our approach in § 3.1, and the technical details in § 4.1. Figure 3 presents the overview of ViLex.

### 3.1. Visual Lexicon

**Approach overview.** ViLex aims to capture high-level semantic representations – such as object categories and layouts – while also preserving rich visual details like styles, patterns, and textures that are difficult or even impossible to describe in natural language.

To accomplish this, we train ViLex through a self-supervised learning pipeline, with a frozen pretrained text-to-image (T2I) diffusion model serving as the source of supervisory signals. This approach enables ViLex to extract visual representations that encompass both semantic-level understanding and intricate visual features. Unlike previous works that directly use diffusion models as feature extractors [3, 19, 35, 79], we take a different approach. In our framework, diffusion models act as decoders in an autoencoder [4, 25, 34, 73] pipeline, which allows us to bake the semantic richness learned by these models into a vision encoder. As a result, ViLex benefits from the detailed and rich visual representations of diffusion models while be-

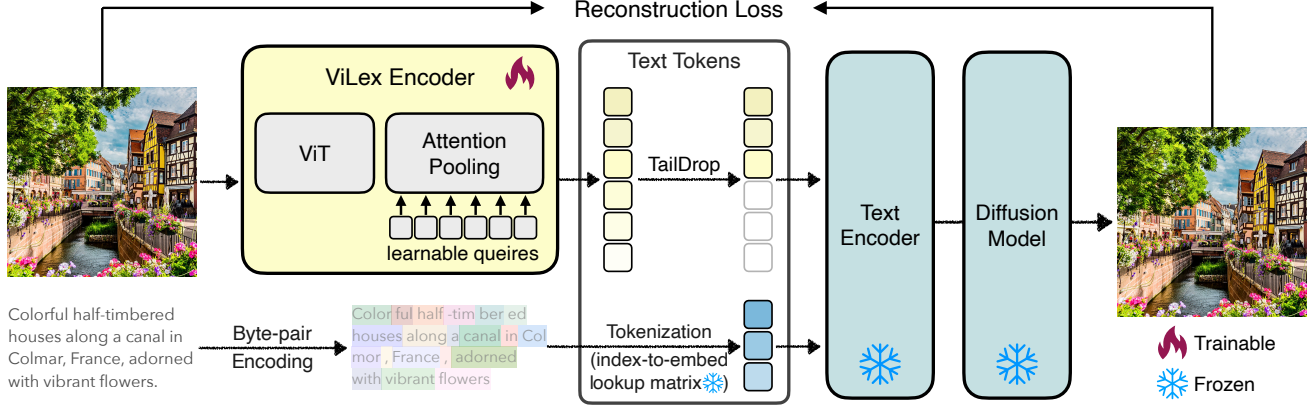


**Figure 3. The pipeline of ViLex:** We learn a Visual Lexicon from a frozen diffusion model using an image reconstruction loss. After training, ViLex can be directly used as the “text-prompt” to a frozen text encoder, *e.g.*, CLIP or T5, enabling the re-creation of semantically similar images without the need for actual text prompts. In addition, during training, we implement the TailDrop strategy, where the last  $k$  tokens are randomly dropped, encouraging earlier tokens in ViLex to carry richer semantic information. ViLex tokens can be utilized independently as “text” tokens for image generation or combined with natural language tokens for prompting T2I diffusion models with both visual and textual cues for multimodal image generation.

ing significantly more lightweight, making it suitable for a broader range of visual scene understanding applications beyond diffusion models’ generative origins.

**Training approach.** As depicted in Figure 3, we employ an autoencoder framework to learn ViLex from a pre-trained text-to-image diffusion model. The overall approach consists of three key components: 1) Image Encoder: A vision transformer (ViT) [16] based image encoder that extracts visual representations from the input image. 2) Image-to-text projection: An attention pooling module that transforms the visual representation into ViLex embeddings within the text space. These embeddings can be independently used as inputs for the frozen text encoder and the subsequent diffusion model, or concatenated with text tokens derived from natural language. 3) Decoder: A pretrained text-to-image diffusion model serves as the decoder in the autoencoder pipeline, generating images from the “text” tokens.

During training, ViLex encoder – which comprises the ViT and the attention pooling module – is optimized via the gradients from image reconstruction loss, while the text-to-image (T2I) model remains frozen throughout the process. After training, ViLex can function as a new “language”, effectively serving as a “text prompt” for frozen text encoders such as CLIP [53] or T5 [54]. This enables the generation of semantically similar images without traditional text-based prompts, capturing intricate visual details.

**Represent images as text embeddings.** Since ViLex is designed to serve as text tokens for text-to-image (T2I) diffusion models, we project the  $k$  patch-level representations  $p_i$  of an image  $i$  into the text space using a multi-head cross-attention layer [82], denoted as  $f(\cdot)$ . This layer contains  $n$  learnable queries and uses the  $k$  output patch tokens from

the image encoder as inputs. These  $k$  patch tokens function as both keys and values within the cross-attention mechanism. Through this setup, the model learns to pool the  $k$  patch tokens into ViLex embeddings, denoted as  $v$ , consisting of  $n$  tokens such that  $v_i = f(p_i)$ , as shown in Figure 3.

To illustrate how to implicitly align ViLex embeddings  $v$  with text tokens  $c$  compatible with a pretrained T2I model, let’s first examine how actual text prompts are tokenized. Using Byte-Pair Encoding (BPE) [7, 17, 62] as an example – a tokenizer employed by CLIP [53] – BPE tokenizes text into sub-word units, effectively managing large vocabularies and handling rare or unseen words. The process has two steps: 1. *Tokenization with BPE*: Each input sentence is tokenized using BPE, yielding a sequence of sub-word tokens. For instance, the phrase “hello world” might be tokenized as: tokens = [“hel”, “lo”, “wor”, “ld”]. 2. *Embedding Lookup*: Each sub-word token is mapped to a learned embedding vector via a pre-trained vocabulary lookup matrix  $\mathcal{V}$ . If  $e_i$  denotes the embedding for token  $i$ , each sub-word token with an index  $t_i$  is given by  $e_i = \mathcal{V}[t_i]$ .

The ViLex embeddings  $v$  are trained to be implicitly aligned with the latent space of the lookup matrix  $\mathcal{V}$ , ensuring compatibility with T2I diffusion models. Before feeding ViLex embeddings  $v$  independently or as part of the concatenated token sequence  $[v, c]$  to the T2I model, where  $c$  is the text tokens, we add [BOS] and [EOS] tokens at the beginning and end of the sequence, respectively.

**Text-free guidance for multimodal image generation.** Classifier-Free Guidance (CFG) [26] has been a popular technique to enhance the quality of generated samples of diffusion models by controlling the trade-off between adhering to a given prompt and producing diverse outputs. In



**Figure 4.** ViLex retains more visual details in image-to-image generation compared to DALL·E 3 [5] and DeDiffusion [76], accurately capturing elements such as image style (*e.g.*, the oil painting style in row 1), layout (*e.g.*, the relative position of the corgi and the lighthouse), pose (*e.g.*, the corgi’s stance), and object shapes (*e.g.*, the shape of Van Gogh’s hat). This enables ViLex to produce images that are both semantically and visually consistent with the original input. Even models with text embeddings in a shared language-vision space, like DALL·E 3, capable of generating semantic variations of an image, struggle to faithfully reconstruct the original appearance of the input image. For image-guided DALL·E results, we provide the input images along with the text prompt, “generate an image exactly the same as the input image”. For DeDiffusion, we follow its official image-to-image generation pipeline and use SDXL [52] as the T2I model.

CFG, two sets of samples are generated: one conditioned on the input (*e.g.*, text prompt) and one unconditioned, allowing flexible guidance during the sampling process. Let  $\epsilon_{\theta}(x_t, c)$  denote the noise predicted by the model conditioned on a prompt  $c$  at time  $t$ , and  $\epsilon_{\theta}(x_t)$  denote the unconditioned noise prediction. In CFG, the final prediction  $\epsilon_{\text{guided}}$  is computed as:

$$\epsilon_{\text{guided}} = \epsilon_{\theta}(x_t) + w \cdot (\epsilon_{\theta}(x_t, c) - \epsilon_{\theta}(x_t)) \quad (1)$$

Increasing the guidance scale  $w$  intensifies the prompt adherence, improving fidelity to  $c$  at the cost of diversity.

Inspired by CFG, we introduce Text-Free Guidance (TFG) for our multimodal image generation, balancing the influence of a given text prompt  $c$  and ViLex embedding  $v$ . TFG controls the trade-off by incorporating visual representations from ViLex alongside the text prompt, enabling finer control over generated images. In TFG, we modify the noise prediction by combining the conditioned prediction on the visual and text prompts, denoted as  $\epsilon_{\theta}(x_t, [v, c])$ , and the prediction conditioned on ViLex alone, *i.e.*  $\epsilon_{\theta}(x_t, v)$ . The TFG noise prediction  $\epsilon_{\text{tfg}}$  is then computed as:

$$\epsilon_{\text{tfg}} = \epsilon_{\theta}(x_t, v) + w_{\text{tfg}} \cdot (\epsilon_{\theta}(x_t, [v, c]) - \epsilon_{\theta}(x_t, v)) \quad (2)$$

where  $w_{\text{tfg}}$  is the guidance scale, allowing us to control the impact of ViLex tokens relative to the text prompt. TFG enables multimodal image generation by incorporating both textual and visual cues, *without* requiring T2I model architectural changes or using LoRA [29] adapters.

**TailDrop for dynamic visual token compression.** Different images contain varying amounts of information, this creates a trade-off between representation compactness and

detail richness. We propose a flexible token budget method using a similar masking strategy as in SoundStream [87], which we refer to as TailDrop. Specifically, during training, we randomly drop the last  $k$  ViLex tokens. Since the early tokens are more frequently independently used for image generation, the earlier tokens in ViLex are encouraged to carry richer semantic information. After the model training, during the inference time, users can dynamically adjust the number of tokens in ViLex to suit the needs.

**Training loss.** We adopt the standard diffusion [27, 66, 67] training objective to optimize ViLex, backpropagating the reconstruction loss to update its parameters. In a diffusion model, the denoising objective aims to learn a model  $\epsilon_{\theta}(x_t, t)$  that predicts the noise  $\epsilon$  added to data  $x_0$  at timestep  $t$ . Given a noisy sample  $x_t$ , the objective minimizes the difference between the predicted and true noise:

$$\mathcal{L}_{\text{denoise}} = \mathbb{E}_{x_0, \epsilon, t} [\|\epsilon - \epsilon_{\theta}(x_t, t)\|^2], \quad (3)$$

where  $x_t = \sqrt{\alpha_t}x_0 + \sqrt{1 - \alpha_t}\epsilon$ , with  $\alpha_t$  controlling the noise schedule. This loss enables the model to reverse the diffusion process, gradually reconstructing  $x_0$  from  $x_t$ .

## 4. Experiments

### 4.1. Technical Details

We describe main technical details here and provide the full details in the supplement.

**Text-to-image diffusion model.** Following DeDiffusion [76], we use Imagen [60] as the base text-to-image diffusion model, adapting the U-Net architecture from [49, 57] with 600M parameters, an embedding dimension of 256,



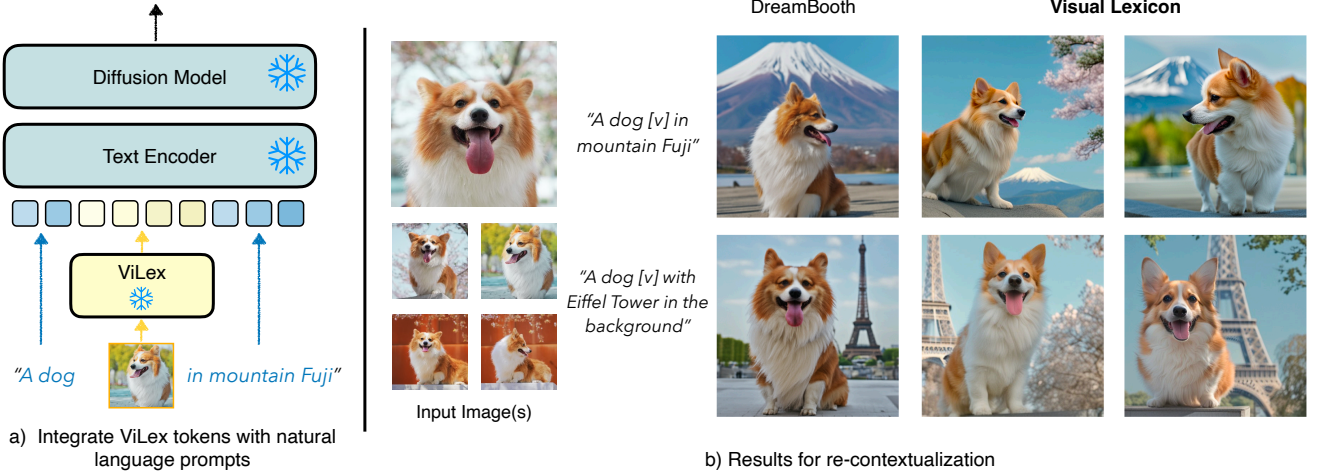


**Figure 5.** ViLex can be seamlessly integrated with natural language prompts for **zero-shot unsupervised image re-contextualization** using a frozen text-to-image (T2I) diffusion model. Unlike DreamBooth [58], ViLex requires no fine-tuning of the T2I model on a set of input images from the same object or modifications to the model architecture (e.g., adding a LoRA [29] adapter). Instead, ViLex is a universal model that enables zero-shot, unsupervised re-contextualization by simply prompting the T2I model with ViLex tokens and corresponding text prompt tokens, just like how we use real words. **a)** The inference pipeline demonstrating image re-contextualization. **b)** Qualitative comparisons with DreamBooth, with DreamBooth results taken from their project page.

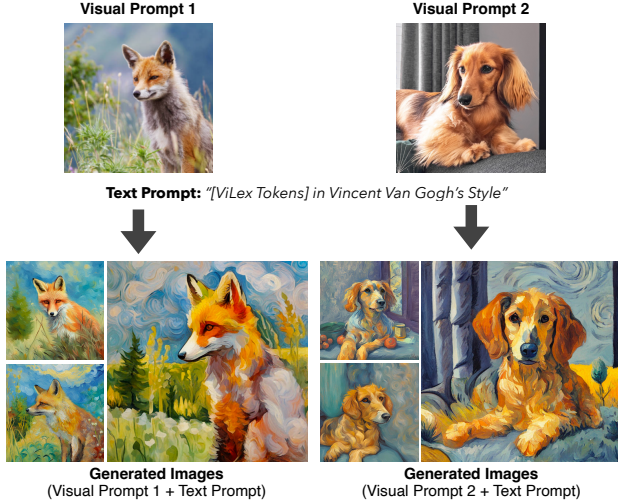


**Figure 6.** ViLex can also support zero-shot unsupervised art rendition via prompting T2I models with ViLex and text prompts.

and an input resolution of  $64 \times 64$ . The text encoder of Imagen is OpenCLIP ViT-H/14 [13, 32] with a vocabulary size of 49408. The U-Net conditions on text embeddings via a pooled embedding vector, which is added to the diffusion timestep embedding. Imagen is further conditioned on the full sequence of text embeddings by incorporating cross-attention over the text embeddings at multiple resolutions.

**Model architecture of ViLex.** ViLex consists of two components: a ViT-based image encoder and a transformer-based attention pooling module. Both components are unfrozen during the training process. For the image encoder,

we use a pretrained SigLIP@224 [88]. SigLIP utilizes ViT-base as the backbone and is pretrained on the WebLI dataset [11] using a sigmoid loss and trained on English image-text pairs, with input images resized to  $224 \times 224$ . The attention pooling module contains  $n$  learnable queries, where  $n \leq 75$ , along with [SOS] and [EOS] tokens to ensure the total token count remains within the 77-context length limit defined by the CLIP text encoder [32, 53]. The attention pooling layer comprises 5 transformer blocks, which are always randomly initialized.

**Model training.** The training data is obtained from WebLI [11], enabling training on either images alone or with image-text pairs. We found that joint image-text training and our TFG are essential for enabling multimodal image generation. However, training without text captions does not negatively impact performance on downstream vision-language tasks. Following [60, 76], we use Adafactor optimizer [63] and a weight decay of 0.01. Training is performed with a batch size of 2048 over 300K steps, which takes approximately 2.5 days on 64 TPUv5 chips. The ViT is initialized with a pretrained SigLIP model and the attention pooling layers are randomly initialized. We use learning rate  $1 \times 10^{-5}$  for the image encoder and  $3 \times 10^{-4}$  for the attention pooling layers, with a cosine learning rate decay and a 10K-step linear warmup. More training details are in the supplement. After training, our ViLex encoder maps an image to ViLex representations. We next evaluate two capabilities of these frozen ViLex representations: image generation and visual understanding.

	T2I	DeDiffusion	ViLex			
			1	4	16	75
FID ( $\downarrow$ )	6.52	3.89	3.65	2.91	2.38	<b>2.07</b>
IS ( $\uparrow$ )	14.06	14.68	15.33	15.42	15.51	<b>15.88</b>

**Table 1.** Even when only using just one continuous token, ViLex outperform the discrete tokens from both DeDiffusion [76] (image→text→image) and the vanilla Imagen [60] (text→image). FID scores on MSCOCO-64×64 were used for image reconstruction comparison across various image generation pipelines, all of which employ Imagen [60] as the base text-to-image diffusion model for fair comparisons. IS refers to inception score.

	DeDiffusion			DALL·E 3		
	layout	semantic	style	layout	semantic	style
vs. ViLex ( $\uparrow$ )	98%	95%	98%	91%	76%	90%

**Table 2. Human studies** on generating semantically and visually similar images using the image-to-image pipeline. We report the percentage of ratings favoring ViLex over DeDiffusion [76] and the image-guided DALL·E 3 [5] in terms of layout, semantic, and style consistency with the input image.

## 4.2. Experiments on Image Generation

**Image-to-image generation** aims to generate similar images given an input image. Feeding our extracted ViLex features on the input image to our T2I model [60] with different diffusion random noise yields re-created images. We compare with two popular models: DALL·E 3 [5] and DeDiffusion [76], both of which convert the input image to explicit texts. DeDiffusion [76] used exactly the same encoder architecture and T2I model as us, giving us an apple-to-apple comparison between our ViLex feature and texts. We conducted both human studies (Table 2) and quantitative metrics on Fréchet Inception Distance (FID) [24] and Inception Score (IS) [68] scores (Table 1).

The quantitative results in Table 1 show that our ViLex efficiently preserves visual information, surpassing the explicit text counterpart [76] even with only 1 token in both FID and IS metrics. We further evaluate the effectiveness of ViLex through human assessments on image-to-image generation tasks. Results in Table 2 indicate that ViLex significantly outperforms the baselines, achieving 98% win rates in layout alignment, 95% in semantic fidelity, and 98% in style preservation against [76]. ViLex also outperforms DALL·E 3. We present qualitative comparisons in Figure 4.

**Zero-shot unsupervised multimodal image generation with identity preserving.** One advantage of mapping images to the word space is to embed images directly into a sentence in an interleaved way. This enables multimodal image generation using a pure text-to-image model without finetuning. In Figure 5, we demonstrate the ability of ViLex to serve as a “language” for multimodal image generation while preserving the object identity in a given image. The conventional approach to this task like DreamBooth [58] re-



**Figure 7. Qualitative results of semantic-level image reconstruction with varying numbers of ViLex tokens.** ViLex tokens enable the reconstruction of semantically similar images even with a single token, effectively capturing high-level semantics such as categories, object counts, and overall poses. As the number of tokens increases to 16, finer details begin to emerge: mid-level features like image styles, colors, and object textures become apparent. With 75 ViLex tokens, the reconstructions achieve high appearance fidelity, incorporating fine-grained details that blend both low-level and high-level information, such as precise object shapes, sizes, and cross-instance relationships.

quires LoRA [29] adapters and a test-time finetuning with a set of images to learn an embedding for object identity which is slow and computationally expensive, while ours directly infers the target identity feature using our encoder. As shown in Figs. 5 and 6, ViLex improves the resulting images by embedding detailed semantic and visual context, producing coherent multimodal results that reflect both the textual prompt and the visual cues provided. We highlight again that our model is not finetuned for this task and does not require a text-time-finetuning like DreamBooth, but simply prompting a standard T2I model with ViLex embeddings and corresponding text prompts.

**When do we need more ViLex tokens?** Figure 7 presents qualitative results of semantic-level image reconstruction with varying numbers of ViLex tokens, illustrating the gradual refinement of visual details as the token count increases. With just 1 token, ViLex effectively captures high-level se-

		Image Captioning					Visual Question Answering						Image Segmentation					Video	
		<i>COCOCap</i>	<i>COCO-35L</i>	<i>TextCap</i>	<i>SciCap-Val</i>	<i>SciCap-Test</i>	<i>VQAv2-Val</i>	<i>TextVQA</i>	<i>OKVQA</i>	<i>SciQA</i>	<i>VizWizQA</i>	<i>GQA</i>	<i>RC-val</i>	<i>RC-testA</i>	<i>RC-testB</i>	<i>RCp-testA</i>	<i>RCp-testB</i>	<i>RCg-test</i>	<i>MSRVTT</i>
Backbone	FID (↓)																		
Original SigLIP	2.54	139.7	138.6	122.1	131.7	135.5	81.4	51.9	57.1	85.9	74.3	64.8	66.2	69.0	63.6	63.3	55.3	59.6	69.4
ViLex SigLIP	<b>2.38</b>	<b>141.5</b>	<b>139.4</b>	<b>124.0</b>	<b>134.3</b>	<b>136.2</b>	<b>81.6</b>	<b>52.9</b>	<b>58.4</b>	<b>87.9</b>	<b>74.9</b>	<b>65.3</b>	<b>67.6</b>	<b>70.0</b>	<b>65.1</b>	<b>65.3</b>	<b>57.3</b>	<b>62.6</b>	<b>70.7</b>

**Table 3. ViLex improves both image understanding and reconstruction capabilities of vision encoders** by fine-tuning them using ViLex’s training approach. Compared with the official SigLIP model [88], ViLex SigLIP, fine-tuned with ViLex approach, demonstrates superior image reconstruction quality (evidenced by a lower FID score) and enhanced visual scene understanding (as shown by improved results on numerous vision-language tasks). We utilize PaliGemma’s [6] framework for linear evaluation, replacing the vision encoder with either the fine-tuned SigLIP in ViLex or the official one, and freeze vision encoder and fine-tune the model on downstream tasks. We use the same hyper-parameters and model architecture for a fair comparison. RC refers to RefCOCO dataset.

mantic information, such as object categories, counts, and poses. As the token count increases to 16, mid-level features, including image styles, colors, and textures, start to emerge, enhancing the overall visual representation. Finally, with 75 tokens, ViLex captures fine-grained details such as precise object shapes, sizes, and intricate cross-instance relationships. For instance, in the third-row image, the two cats’ poses are accurately reconstructed, including their specific positioning and interaction as they cuddle together. These results demonstrate ViLex’ adaptability, providing users with the flexibility to balance semantic richness and visual detail based on the application requirements.

### 4.3. Experiments on Image Understanding

We next verify that our frozen ViLex features can be directly used for understanding tasks, by feeding them to a large language model [69]. We use PaliGemma [6] as our visual-language model (VLM) architecture. PaliGemma [6] is an open-source VLM with a SigLIP-So400m [88] vision encoder and a Gemma-2B [69] language model. To use ViLex in PaliGemma, we replace the SigLIP [88] vision encoder with our ViLex encoder. In all our following experiments, we don’t finetune our ViLex encoder, and only finetune the following large language model [69] to adapt to the tasks following the PaliGemma transfer design [6].

**Improving vision encoders over SigLip.** We first conduct a comparison between the visual encoder learned from our ViLex pretraining and the popular SigLip [88]. To ensure a fair comparison in terms of the architecture and the number of tokens, we use our features right after the ViT-encoder without the pooling layer. Table 3 shows the results. We also show the image reconstruction FID. The results show that ViLex feature consistently improves the strong SigLip model by over 1 point margin on a variety number of vision-language tasks, including image captioning, referring segmentation, and video understanding. This shows that ViLex can effectively upgrade existing vision encoders to perform better in both reconstruction and understanding.

**Vision-language tasks.** ViLex can also serve as a strong

Image Encoder	COCOcap	TextCaps	TextVQA	OKVQA	SciQA	RC-val	RCp-testA	RCg-test
VAE	61.4	15.0	12.9	33.3	82.1	19.5	12.1	13.8
ViLex SigLIP	<b>141.5</b>	<b>124.0</b>	<b>52.9</b>	<b>57.5</b>	<b>87.9</b>	<b>67.2</b>	<b>65.3</b>	<b>62.6</b>
ViLex	<b>142.8</b>	<b>137.7</b>	<b>59.4</b>	<b>58.3</b>	<b>88.6</b>	<b>70.9</b>	<b>69.2</b>	<b>65.9</b>

**Table 4. Improving vision-language models with ViLex tokens.** Concatenating ViLex tokens with SigLIP patch tokens enhances the performance of vision-language models across diverse downstream tasks, such as image captioning, visual question answering, and image segmentation, with a modest token increase of only 25% (from 256 to 336). **Pixel-reconstruction or semantic-reconstruction?** Although VAE can preserve pixel-level details during image reconstruction, its lack of semantic richness results in significantly poorer performance in vision-language modeling compared to ViLex. We use PaliGemma as the base VLM model.

vision encoder for vision-language models. ViLex tokens are inherently ready to use for vision-language frameworks, therefore, they can be directly utilized without requiring fine-tuning the image encoder. Despite freezing the image encoder—including both the ViT and attention pooling layers—we observed significant performance improvements across various tasks, such as visual question answering, image captioning, and referring expression segmentation, as demonstrated in Table 4 and Table 5. Following prior works like QwenVL-7B, LLaVA1.5-13B, LLaVA1.6-13B [1, 41, 42], we adopt a multi-grid input strategy for extracting visual representations to ensure a fair comparison with these methods. However, unlike these methods, which increase the overall number of tokens by 2~5 times, we use only 16 ViLex tokens per grid. This results in only 25% increase in token count (adding just 80 tokens) while achieving substantial performance improvements and setting new state-of-the-art results on multiple VQA benchmarks.

**Pixel-reconstruction or semantic-reconstruction?** Although VAE [25, 34, 56] excels at preserving pixel-level details during image reconstruction, its [56] lack of seman-



Model	#toks	VQA <sub>v2</sub>	SciQA	VizWizQA	GQA
<b>Freeze image encoder</b>					
PaliGemma-2B (SigLIP@224)	256	81.4	85.9	74.3	64.8
PaliGemma-2B (ViLex @224)	336	<b>83.6</b>	<b>88.6</b>	<b>75.8</b>	<b>65.7</b>
<b>Fine-tune image encoder</b>					
LLaVA1.5-7B (CLIP@224)[41]	576	78.5*	66.8	50.0	62.0*
LLaVA1.5-13B (CLIP@224)[41]	576	80.0*	71.6	53.6	62.0*
VILA-13B (CLIP@336)[39]	576	80.8*	73.7	60.6	63.3*
QwenVL-7B (CLIP@448)[1]	1024	78.8*	67.1	38.9	57.5*
LLaVA1.5-13B (CLIP@336) <sup>HD</sup> [41]	1280	81.8*	71.0	57.5	63.3*
LLaVA1.6-13B (CLIP@384) <sup>HD</sup> [42]	1280	81.8*	70.2	-	64.2*

**Table 5. ViLex can be a strong vision encoder for vision-language tasks.** Using the *lowest image resolution*, *fewer tokens per image*, the *smallest LLM model*, and *without fine-tuning image encoder*, our ViLex—integrated into PaliGemma as the image encoder—achieves SOTA performance across multiple visual question answering tasks. \*: The training images from the datasets are utilized during model training or for fine-tuning the model.

tic richness leads to substantially poorer performance (often >8 times lower) in vision-language modeling compared to ViLex, as demonstrated in Table 4.

## 5. Conclusions

We introduce ViLex, a visual lexicon that maps images directly into the text space, while effectively preserving complex visual details that are difficult to express in natural language. Our representation can be seamlessly integrated into text prompts from natural language for both multimodal image generation and downstream vision-language tasks. ViLex can also improve both image understanding and reconstruction capabilities of pretrained vision encoders by fine-tuning them using ViLex’s training approach.

**Acknowledgment.** We sincerely thank Alexei A. Efros, Ren Ng, David Minnen, Lijun Yu, Xiuye Gu, Haiwen (Haven) Feng, Renhao Wang, Baifeng Shi, and Tony Long Lian for their insightful discussions and valuable feedback on our paper. We also thank Chen Wei for her assistance in reproducing the baseline results.

## References

- [1] Jinze Bai, Shuai Bai, Shusheng Yang, Shijie Wang, Sinan Tan, Peng Wang, Junyang Lin, Chang Zhou, and Jingren Zhou. Qwen-vl: A frontier large vision-language model with versatile abilities. *arXiv:2308.12966*, 2023. 8, 9
- [2] Hangbo Bao, Li Dong, Songhao Piao, and Furu Wei. BEiT: BERT pre-training of image transformers. In *ICLR*, 2022. 3
- [3] Dmitry Baranchuk, Andrey Voynov, Ivan Rubachev, Valentin Khurlov, and Artem Babenko. Label-efficient semantic segmentation with diffusion models. In *ICLR*, 2022. 2, 3

- [4] Yoshua Bengio, Li Yao, Guillaume Alain, and Pascal Vincent. Generalized denoising auto-encoders as generative models. *Advances in neural information processing systems*, 26, 2013. 2, 3
- [5] James Betker, Gabriel Goh, Li Jing, Tim Brooks, Jianfeng Wang, Linjie Li, Long Ouyang, Juntang Zhuang, Joyce Lee, Yufei Guo, et al. Improving image generation with better captions. *Computer Science*. <https://cdn.openai.com/papers/dall-e-3.pdf>, 2(3):8, 2023. 2, 5, 7
- [6] Lucas Beyer, Andreas Steiner, André Susano Pinto, Alexander Kolesnikov, Xiao Wang, Daniel Salz, Maxim Neumann, Ibrahim Alabdulmohsin, Michael Tschannen, Emanuele Bugliarello, et al. Paligemma: A versatile 3b vlm for transfer. *arXiv:2407.07726*, 2024. 2, 3, 8, 13, 14
- [7] Tom B Brown. Language models are few-shot learners. *arXiv preprint arXiv:2005.14165*, 2020. 4
- [8] Mathilde Caron, Hugo Touvron, Ishan Misra, Hervé Jégou, Julien Mairal, Piotr Bojanowski, and Armand Joulin. Emerging properties in self-supervised vision transformers. In *CVPR*, 2021. 1, 3
- [9] Mark Chen, Alec Radford, Rewon Child, Jeffrey Wu, Heewoo Jun, David Luan, and Ilya Sutskever. Generative pre-training from pixels. In *International conference on machine learning*, pages 1691–1703. PMLR, 2020. 3
- [10] Xinlei Chen, Hao Fang, Tsung-Yi Lin, Ramakrishna Vedantam, Saurabh Gupta, Piotr Dollár, and C Lawrence Zitnick. Microsoft coco captions: Data collection and evaluation server. *arXiv:1504.00325*, 2015. 2
- [11] Xi Chen, Xiao Wang, Soravit Changpinyo, AJ Piergiovanni, Piotr Padlewski, Daniel Salz, Sebastian Goodman, Adam Grycner, Basil Mustafa, Lucas Beyer, et al. Pali: A jointly-scaled multilingual language-image model. *arXiv:2209.06794*, 2022. 6, 13
- [12] Xinlei Chen, Zhuang Liu, Saining Xie, and Kaiming He. Deconstructing denoising diffusion models for self-supervised learning. *arXiv:2401.14404*, 2024. 3
- [13] Mehdi Cherti, Romain Beaumont, Ross Wightman, Mitchell Wortsman, Gabriel Ilharco, Cade Gordon, Christoph Schuhmann, Ludwig Schmidt, and Jenia Jitsev. Reproducible scaling laws for contrastive language-image learning. In *CVPR*, 2023. 6, 13
- [14] Jia Deng, Wei Dong, Richard Socher, Li-Jia Li, Kai Li, and Li Fei-Fei. Imagenet: A large-scale hierarchical image database. In *CVPR*, 2009. 1, 3
- [15] Jeff Donahue and Karen Simonyan. Large scale adversarial representation learning. *NeurIPS*, 32, 2019. 3
- [16] Alexey Dosovitskiy, Lucas Beyer, Alexander Kolesnikov, Dirk Weissenborn, Xiaohua Zhai, Thomas Unterthiner, Mostafa Dehghani, Matthias Minderer, Georg Heigold, Sylvain Gelly, Jakob Uszkoreit, and Neil Houlsby. An image is worth 16x16 words: Transformers for image recognition at scale. *ICLR*, 2021. 4
- [17] Philip Gage. A new algorithm for data compression. *The C Users Journal*, 12(2):23–38, 1994. 4
- [18] Rinon Gal, Yuval Alaluf, Yuval Atzmon, Or Patashnik, Amit H Bermano, Gal Chechik, and Daniel Cohen-Or. An image is worth one word: Personalizing text-to-image generation using textual inversion. *ICLR*, 2023. 3, 16

- [19] Yulu Gan, Sungwoo Park, Alexander Marcel Schubert, Anthony Philippakis, and Ahmed Alaa. Instructcv: Instruction-tuned text-to-image diffusion models as vision generalists. In *The Twelfth International Conference on Learning Representations*, 2024. 2, 3
- [20] Rohit Girdhar, Alaaeldin El-Nouby, Zhuang Liu, Mannat Singh, Kalyan Vasudev Alwala, Armand Joulin, and Ishan Misra. Imagebind: One embedding space to bind them all. In *Proceedings of the IEEE/CVF Conference on Computer Vision and Pattern Recognition*, pages 15180–15190, 2023. 3
- [21] Yash Goyal, Tejas Khot, Douglas Summers-Stay, Dhruv Batra, and Devi Parikh. Making the v in vqa matter: Elevating the role of image understanding in visual question answering. In *CVPR*, 2017. 2, 13
- [22] Danna Gurari, Qing Li, Abigale J Stangl, Anhong Guo, Chi Lin, Kristen Grauman, Jiebo Luo, and Jeffrey P Bigham. Vizwiz grand challenge: Answering visual questions from blind people. In *Proceedings of the IEEE conference on computer vision and pattern recognition*, pages 3608–3617, 2018. 13
- [23] Kaiming He, Xinlei Chen, Saining Xie, Yanghao Li, Piotr Dollár, and Ross Girshick. Masked autoencoders are scalable vision learners. In *CVPR*, 2022. 1, 2, 3
- [24] Martin Heusel, Hubert Ramsauer, Thomas Unterthiner, Bernhard Nessler, and Sepp Hochreiter. Gans trained by a two time-scale update rule converge to a local nash equilibrium. *Advances in neural information processing systems*, 30, 2017. 7
- [25] Geoffrey E Hinton and Richard Zemel. Autoencoders, minimum description length and helmholtz free energy. *Advances in neural information processing systems*, 6, 1993. 2, 3, 8
- [26] Jonathan Ho and Tim Salimans. Classifier-free diffusion guidance. In *NeurIPS 2021 Workshop on Deep Generative Models and Downstream Applications*, 2021. 4
- [27] Jonathan Ho, Ajay Jain, and Pieter Abbeel. Denoising diffusion probabilistic models. *Advances in neural information processing systems*, 33:6840–6851, 2020. 2, 5
- [28] Ting-Yao Hsu, C Lee Giles, and Ting-Hao’Kenneth’ Huang. Scicap: Generating captions for scientific figures. *arXiv preprint arXiv:2110.11624*, 2021. 13
- [29] Edward J Hu, Yelong Shen, Phillip Wallis, Zeyuan Allen-Zhu, Yuanzhi Li, Shean Wang, Lu Wang, and Weizhu Chen. Lora: Low-rank adaptation of large language models. *arXiv:2106.09685*, 2021. 5, 6, 7, 16
- [30] Drew A Hudson and Christopher D Manning. Gqa: A new dataset for real-world visual reasoning and compositional question answering. In *Proceedings of the IEEE/CVF conference on computer vision and pattern recognition*, pages 6700–6709, 2019. 14
- [31] Drew A Hudson, Daniel Zoran, Mateusz Malinowski, Andrew K Lampinen, Andrew Jaegle, James L McClelland, Loic Matthey, Felix Hill, and Alexander Lerchner. Soda: Bottleneck diffusion models for representation learning. In *CVPR*, 2024. 3
- [32] Gabriel Ilharco, Mitchell Wortsman, Ross Wightman, Cade Gordon, Nicholas Carlini, Rohan Taori, Achal Dave, Vaishal Shankar, Hongseok Namkoong, John Miller, Hananeh Hajishirzi, Ali Farhadi, and Ludwig Schmidt. Openclip, 2021. 6, 13
- [33] Sahar Kazemzadeh, Vicente Ordonez, Mark Matten, and Tamara Berg. Referitgame: Referring to objects in photographs of natural scenes. In *Proceedings of the 2014 conference on empirical methods in natural language processing (EMNLP)*, pages 787–798, 2014. 14
- [34] Diederik P Kingma. Auto-encoding variational bayes. *arXiv preprint arXiv:1312.6114*, 2013. 1, 2, 3, 8
- [35] Alexander C Li, Mihir Prabhudesai, Shivam Duggal, Ellis Brown, and Deepak Pathak. Your diffusion model is secretly a zero-shot classifier. In *Proceedings of the IEEE/CVF International Conference on Computer Vision*, pages 2206–2217, 2023. 2, 3
- [36] Bo Li, Yuanhan Zhang, Dong Guo, Renrui Zhang, Feng Li, Hao Zhang, Kaichen Zhang, Yanwei Li, Ziwei Liu, and Chunyuan Li. Llava-onevision: Easy visual task transfer. *arXiv:2408.03326*, 2024. 3
- [37] Junnan Li, Dongxu Li, Caiming Xiong, and Steven Hoi. Blip: Bootstrapping language-image pre-training for unified vision-language understanding and generation. In *ICLR*. PMLR, 2022. 3
- [38] Xiang Li, Hao Chen, Kai Qiu, Jason Kuen, Jiuxiang Gu, Bhiksha Raj, and Zhe Lin. Imagefolder: Autoregressive image generation with folded tokens. *arXiv:2410.01756*, 2024. 3
- [39] Ji Lin, Hongxu Yin, Wei Ping, Pavlo Molchanov, Mohammad Shoeybi, and Song Han. Vila: On pre-training for visual language models. In *CVPR*, 2024. 9
- [40] Tsung-Yi Lin, Michael Maire, Serge Belongie, James Hays, Pietro Perona, Deva Ramanan, Piotr Dollár, and C Lawrence Zitnick. Microsoft coco: Common objects in context. In *ECCV*, 2014. 13, 15
- [41] Haotian Liu, Chunyuan Li, Yuheng Li, and Yong Jae Lee. Improved baselines with visual instruction tuning. In *CVPR*, 2024. 8, 9
- [42] Haotian Liu, Chunyuan Li, Yuheng Li, Bo Li, Yuanhan Zhang, Sheng Shen, and Yong Jae Lee. Llava-next: Improved reasoning, ocr, and world knowledge, 2024. 8, 9
- [43] Pan Lu, Swaroop Mishra, Tanglin Xia, Liang Qiu, Kai-Wei Chang, Song-Chun Zhu, Oyvind Tafjord, Peter Clark, and Ashwin Kalyan. Learn to explain: Multimodal reasoning via thought chains for science question answering. *Advances in Neural Information Processing Systems*, 35:2507–2521, 2022. 13
- [44] Shweta Mahajan, Tanzila Rahman, Kwang Moo Yi, and Leonid Sigal. Prompting hard or hardly prompting: Prompt inversion for text-to-image diffusion models. In *CVPR*, 2024. 3
- [45] Junhua Mao, Jonathan Huang, Alexander Toshev, Oana Camburu, Alan L Yuille, and Kevin Murphy. Generation and comprehension of unambiguous object descriptions. In *Proceedings of the IEEE conference on computer vision and pattern recognition*, pages 11–20, 2016. 14
- [46] Kenneth Marino, Mohammad Rastegari, Ali Farhadi, and Roozbeh Mottaghi. Ok-vqa: A visual question answering

- benchmark requiring external knowledge. In *Proceedings of the IEEE/cvf conference on computer vision and pattern recognition*, pages 3195–3204, 2019. 13
- [47] Fabian Mentzer, David Minnen, Eirikur Agustsson, and Michael Tschannen. Finite scalar quantization: Vq-vae made simple. *ICLR*, 2024. 3
- [48] Ron Mokady, Amir Hertz, Kfir Aberman, Yael Pritch, and Daniel Cohen-Or. Null-text inversion for editing real images using guided diffusion models. In *Proceedings of the IEEE/CVF Conference on Computer Vision and Pattern Recognition*, pages 6038–6047, 2023. 3
- [49] Alexander Quinn Nichol and Prafulla Dhariwal. Improved denoising diffusion probabilistic models. In *ICML*. PMLR, 2021. 5, 13
- [50] Maxime Oquab, Timothée Darcet, Théo Moutakanni, Huy Vo, Marc Szafraniec, Vasil Khalidov, Pierre Fernandez, Daniel Haziza, Francisco Massa, Alaaeldin El-Nouby, et al. Dinov2: Learning robust visual features without supervision. *arXiv:2304.07193*, 2023. 1, 3
- [51] Or Patashnik, Zongze Wu, Eli Shechtman, Daniel Cohen-Or, and Dani Lischinski. Styleclip: Text-driven manipulation of stylegan imagery. In *Proceedings of the IEEE/CVF international conference on computer vision*, pages 2085–2094, 2021. 3
- [52] Dustin Podell, Zion English, Kyle Lacey, Andreas Blattmann, Tim Dockhorn, Jonas Müller, Joe Penna, and Robin Rombach. Sdxl: Improving latent diffusion models for high-resolution image synthesis. In *The Twelfth International Conference on Learning Representations*, 2023. 3, 5
- [53] Alec Radford, Jong Wook Kim, Chris Hallacy, Aditya Ramesh, Gabriel Goh, Sandhini Agarwal, Girish Sastry, Amanda Askell, Pamela Mishkin, Jack Clark, et al. Learning transferable visual models from natural language supervision. In *ICLR*, 2021. 1, 2, 3, 4, 6, 13
- [54] Colin Raffel, Noam Shazeer, Adam Roberts, Katherine Lee, Sharan Narang, Michael Matena, Yanqi Zhou, Wei Li, and Peter J Liu. Exploring the limits of transfer learning with a unified text-to-text transformer. *Journal of machine learning research*, 2020. 2, 4
- [55] Aditya Ramesh, Prafulla Dhariwal, Alex Nichol, Casey Chu, and Mark Chen. Hierarchical text-conditional image generation with clip latents. *arXiv preprint arXiv:2204.06125*, 2022. 1
- [56] Robin Rombach, Andreas Blattmann, Dominik Lorenz, Patrick Esser, and Björn Ommer. High-resolution image synthesis with latent diffusion models. In *CVPR*, 2022. 2, 3, 8
- [57] Olaf Ronneberger, Philipp Fischer, and Thomas Brox. U-net: Convolutional networks for biomedical image segmentation. In *MICCAI*, 2015. 5, 13
- [58] Nataniel Ruiz, Yuanzhen Li, Varun Jampani, Yael Pritch, Michael Rubinstein, and Kfir Aberman. Dreambooth: Fine tuning text-to-image diffusion models for subject-driven generation. In *CVPR*, 2023. 2, 3, 6, 7, 16
- [59] Nataniel Ruiz, Yuanzhen Li, Varun Jampani, Wei Wei, Tingbo Hou, Yael Pritch, Neal Wadhwa, Michael Rubinstein, and Kfir Aberman. Hyperdreambooth: Hypernetworks for fast personalization of text-to-image models. In *CVPR*, 2024. 3, 16
- [60] Chitwan Saharia, William Chan, Saurabh Saxena, Lala Li, Jay Whang, Emily L Denton, Kamyar Ghasemipour, Raphael Gontijo Lopes, Burcu Karagol Ayan, Tim Salimans, et al. Photorealistic text-to-image diffusion models with deep language understanding. *Advances in neural information processing systems*, 35:36479–36494, 2022. 1, 2, 3, 5, 6, 7, 13
- [61] Tim Salimans and Jonathan Ho. Progressive distillation for fast sampling of diffusion models. In *ICLR*, 2021. 13
- [62] Rico Sennrich. Neural machine translation of rare words with subword units. *arXiv preprint arXiv:1508.07909*, 2015. 4
- [63] Noam Shazeer and Mitchell Stern. Adafactor: Adaptive learning rates with sublinear memory cost. In *ICML*. PMLR, 2018. 6, 13
- [64] Oleksii Sidorov, Ronghang Hu, Marcus Rohrbach, and Amanpreet Singh. Textcaps: a dataset for image captioning with reading comprehension. In *Computer Vision—ECCV 2020: 16th European Conference, Glasgow, UK, August 23–28, 2020, Proceedings, Part II 16*, pages 742–758. Springer, 2020. 13
- [65] Amanpreet Singh, Vivek Natarajan, Meet Shah, Yu Jiang, Xinlei Chen, Dhruv Batra, Devi Parikh, and Marcus Rohrbach. Towards vqa models that can read. In *Proceedings of the IEEE/CVF conference on computer vision and pattern recognition*, pages 8317–8326, 2019. 13
- [66] Jascha Sohl-Dickstein, Eric Weiss, Niru Maheswaranathan, and Surya Ganguli. Deep unsupervised learning using nonequilibrium thermodynamics. In *ICML*. PMLR, 2015. 5
- [67] Yang Song and Stefano Ermon. Generative modeling by estimating gradients of the data distribution. *Advances in neural information processing systems*, 32, 2019. 5
- [68] Christian Szegedy, Vincent Vanhoucke, Sergey Ioffe, Jon Shlens, and Zbigniew Wojna. Rethinking the inception architecture for computer vision. In *Proceedings of the IEEE conference on computer vision and pattern recognition*, pages 2818–2826, 2016. 7
- [69] Gemma Team, Thomas Mesnard, Cassidy Hardin, Robert Dadashi, Surya Bhupatiraju, Shreya Pathak, Laurent Sifre, Morgane Rivi re, Mihir Sanjay Kale, Juliette Love, et al. Gemma: Open models based on gemini research and technology. *arXiv preprint arXiv:2403.08295*, 2024. 8
- [70] Ashish V Thapliyal, Jordi Pont-Tuset, Xi Chen, and Radu Soricut. Crossmodal-3600: A massively multilingual multimodal evaluation dataset. *arXiv preprint arXiv:2205.12522*, 2022. 13
- [71] Keyu Tian, Yi Jiang, Zehuan Yuan, Bingyue Peng, and Liwei Wang. Visual autoregressive modeling: Scalable image generation via next-scale prediction. *NeurIPS*, 2024. 3
- [72] Yonglong Tian, Dilip Krishnan, and Phillip Isola. Contrastive multiview coding. In *ECCV*, 2020. 3
- [73] Pascal Vincent, Hugo Larochelle, Yoshua Bengio, and Pierre-Antoine Manzagol. Extracting and composing robust features with denoising autoencoders. In *Proceedings of the*



- 25th international conference on Machine learning, pages 1096–1103, 2008. 2, 3
- [74] Wenxuan Wang, Quan Sun, Fan Zhang, Yepeng Tang, Jing Liu, and Xinlong Wang. Diffusion feedback helps clip see better. *arXiv:2407.20171*, 2024. 3
- [75] Xudong Wang, Ziwei Liu, and Stella X Yu. Unsupervised feature learning by cross-level instance-group discrimination. In *CVPR*, 2021. 3
- [76] Chen Wei, Chenxi Liu, Siyuan Qiao, Zhishuai Zhang, Alan Yuille, and Jiahui Yu. De-diffusion makes text a strong cross-modal interface. In *Proceedings of the IEEE/CVF Conference on Computer Vision and Pattern Recognition*, pages 13492–13503, 2024. 2, 3, 5, 6, 7, 13
- [77] Zhirong Wu, Yuanjun Xiong, Stella X Yu, and Dahua Lin. Unsupervised feature learning via non-parametric instance discrimination. In *CVPR*, 2018. 3
- [78] Jun Xu, Tao Mei, Ting Yao, and Yong Rui. Msr-vtt: A large video description dataset for bridging video and language. In *CVPR*, 2016. 2, 14, 16
- [79] Jiarui Xu, Sifei Liu, Arash Vahdat, Wonmin Byeon, Xiaolong Wang, and Shalini De Mello. Open-vocabulary panoptic segmentation with text-to-image diffusion models. In *Proceedings of the IEEE/CVF Conference on Computer Vision and Pattern Recognition*, pages 2955–2966, 2023. 2, 3
- [80] Xingyi Yang and Xinchao Wang. Diffusion model as representation learner. In *ICCV*, 2023. 3
- [81] Jiahui Yu, Xin Li, Jing Yu Koh, Han Zhang, Ruoming Pang, James Qin, Alexander Ku, Yuanzhong Xu, Jason Baldridge, and Yonghui Wu. Vector-quantized image modeling with improved vqgan. *ICLR*, 2022. 3
- [82] Jiahui Yu, Zirui Wang, Vijay Vasudevan, Legg Yeung, Mojtaba Seyedhosseini, and Yonghui Wu. Coca: Contrastive captioners are image-text foundation models. *Transactions on Machine Learning Research*, 2022. 4, 15, 16
- [83] Licheng Yu, Patrick Poirson, Shan Yang, Alexander C Berg, and Tamara L Berg. Modeling context in referring expressions. In *ECCV*, 2016. 2, 14
- [84] Lijun Yu, Yong Cheng, Zhiruo Wang, Vivek Kumar, Wolfgang Macherey, Yanping Huang, David Ross, Irfan Essa, Yonatan Bisk, Ming-Hsuan Yang, et al. Spae: Semantic pyramid autoencoder for multimodal generation with frozen llms. *NeurIPS*, 2024. 3
- [85] Lijun Yu, José Lezama, Nitesh B Gundavarapu, Luca Versari, Kihyuk Sohn, David Minnen, Yong Cheng, Vignesh Birodkar, Agrim Gupta, Xiuye Gu, et al. Language model beats diffusion—tokenizer is key to visual generation. *ICLR*, 2024. 3
- [86] Qihang Yu, Mark Weber, Xueqing Deng, Xiaohui Shen, Daniel Cremers, and Liang-Chieh Chen. An image is worth 32 tokens for reconstruction and generation. *NeurIPS*, 2024. 1, 3
- [87] Neil Zeghidour, Alejandro Luebs, Ahmed Omran, Jan Skoglund, and Marco Tagliasacchi. Soundstream: An end-to-end neural audio codec. *IEEE/ACM Transactions on Audio, Speech, and Language Processing*, 2021. 5
- [88] Xiaohua Zhai, Basil Mustafa, Alexander Kolesnikov, and Lucas Beyer. Sigmoid loss for language image pre-training. In *CVPR*, 2023. 2, 3, 6, 8, 13, 15, 16
- [89] Yue Zhao, Yuanjun Xiong, and Philipp Krähenbühl. Image and video tokenization with binary spherical quantization. *arXiv:2406.07548*, 2024. 3

# Visual Lexicon: Rich Image Features in Language Space

## Supplementary Material

### A1. Technical Details

We introduced the main technical and implementation details of our ViLex model in the main paper, here we provide a more comprehensive explanation.

**Text-to-image diffusion model.** Following DeDiffusion [76], we use Imagen [60] as the base text-to-image diffusion model, adapting the U-Net architecture from [49, 57] with 600M parameters, an embedding dimension of 256, and an input resolution of  $64 \times 64$ . The text encoder of Imagen is OpenCLIP ViT-H/14 [13, 32] with a vocabulary size of 49408. The U-Net conditions on text embeddings via a pooled embedding vector, which is added to the diffusion timestep embedding. Imagen is further conditioned on the full sequence of text embeddings by incorporating cross-attention over the text embeddings at multiple resolutions. The Imagen model uses  $v$ -prediction [61] as its objective, with a batch size of 2048, and is trained for 3 million steps. As a baseline model, Imagen achieves an FID of 6.52 on 30K  $64 \times 64$  MS-COCO 2014 validation images [60]. During image generation inference, we use a super-resolution model, such as an SDXL upsampler, to upsample the image resolution from  $64 \times 64$  to  $512 \times 512$  for better visualizations.

**Model architecture of ViLex.** ViLex consists of two components: a ViT-based image encoder and a transformer-based attention pooling module. Both components are unfrozen during the training process. For the image encoder, we use a pretrained SigLIP-So400M@224 [88]. SigLIP utilizes ViT-base as the backbone and is pretrained on the WebLI dataset [11] using a sigmoid loss and trained on English image-text pairs, with input images resized to  $224 \times 224$ . The model architecture of the ViT-base is shape-optimized on 400M training samples for improving the model efficiency and speed. In our method, the attention pooler is implemented as a single multi-head attention layer with learnable queries, using the encoder output as both keys and values. This allows the attention pooling module to effectively aggregate embeddings of varying lengths. The attention pooling module contains  $n$  learnable queries, where  $n \leq 75$ , along with [SOS] and [EOS] tokens to ensure the total token count remains within the 77-context length limit defined by the CLIP text encoder [32, 53]. The attention pooling layer comprises 5 transformer blocks, which are always randomly initialized.

**Model training.** The training data is obtained from WebLI [11], enabling training on either images alone or with image-text pairs. We found that joint image-text training and our TFG are essential for enabling multimodal image generation. However, training without text captions does

not negatively impact performance on downstream vision-language tasks. Following [60, 76], we use Adafactor optimizer [63] and a weight decay of 0.01. Training is performed with a batch size of 2048 over 300K steps, which takes approximately 2.5 days on 64 TPUv5 chips. We found that double the training steps (from 300k to 600k) can further improve the model performance on increasing the performance of a pretrained vision encoder. The ViT is initialized with a pretrained SigLIP model and the attention pooling layers are randomly initialized. We use learning rate  $1 \times 10^{-5}$  for the image encoder and  $3 \times 10^{-4}$  for the attention pooling layers, with a cosine learning rate decay and a 10K-step linear warmup, and a weight decay of 0.01. After training, our ViLex encoder maps an image to ViLex representations. We next evaluate two capabilities of these frozen ViLex representations: image generation and visual understanding.

**PaliGemma experiments.** To evaluate the effectiveness of the proposed ViLex approach in enhancing a pretrained vision encoder for vision-language tasks, we integrate our vision encoder into the PaliGemma [6] framework and replace the vision encoder with either the fine-tuned SigLIP-So400M [88] from ViLex or the official version without model fine-tuning, freezing the vision encoder and fine-tuning the model on downstream tasks. Following PaliGemma’s official pipeline, we transfer the model to a variety of individual academic benchmarks using a unified transfer approach with minimal hyperparameter tuning. To ensure fair comparison, we applied the same hyperparameter sweeping strategy for both the baseline and our fine-tuned vision encoder, reporting the best results for each. This structured approach allows us to fairly assess the impact of the proposed ViLex method on a wide range of vision-language tasks. The sweeping parameters for these tasks are as follows: COCOCap [40] (COCO image captioning task) and COCO-35L [70] (COCO captions translated in 35 languages): learning rate (4e-6, 5e-6, 6e-6), epochs (5, 10), dropout (0, 0.02, 0.05). TextCaps [64] (image captioning with reading comprehension): learning rate (4e-6, 6e-6), and training epochs (5, 10). For SciCaps [28] (captions for scientific figures): learning rate (6e-5, 7e-5), dropout (0.1, 0.2), and label smoothing (0.1, 0.2). For VQAv2 [21] (visual question answering): label smoothing (0.0, 0.1), dropout (0.0, 0.1), and weight decay (0, 1e-6). For TextVQA [65] (visual reasoning based on text in images): learning rate (4e-6, 6e-6). For OKVQA [46] (outside knowledge VQA), ScienceQA [43] (science question answering), and VizWizVQA [22] (VQA from people who are blind): learning rate (8e-6, 1e-5), and dropout (0.0, 0.02).

Backbone	#steps	Image Captioning					Visual Question Answering						Image Segmentation					Video	
		COCOCap	COCO-35L	TextCap	SciCap-Val	SciCap-Test	VQAv2-Val	TextVQA	OKVQA	SciQA	VizWizQA	GQA	RC-val	RC-testA	RC-testB	RCp-testA	RCp-testB	RCg-test	MSRVTT
Original SigLIP	-	139.7	138.6	122.1	131.7	135.5	81.4	51.9	57.1	85.9	74.3	64.8	66.2	69.0	63.6	63.3	55.3	59.6	69.4
ViLex SigLIP	150k	<b>140.5</b>	<b>138.8</b>	<b>122.3</b>	<b>132.6</b>	<b>135.5</b>	<b>81.4</b>	<b>52.1</b>	<b>57.3</b>	<b>86.1</b>	<b>74.5</b>	<b>65.1</b>	<b>66.5</b>	<b>69.3</b>	<b>64.2</b>	<b>64.1</b>	<b>55.6</b>	<b>60.2</b>	<b>70.6</b>
ViLex SigLIP	600k	<b>141.5</b>	<b>140.0</b>	<b>124.0</b>	<b>134.3</b>	<b>136.1</b>	<b>81.8</b>	<b>52.7</b>	<b>58.3</b>	<b>89.3</b>	<b>75.0</b>	<b>65.4</b>	<b>67.5</b>	<b>69.7</b>	<b>65.6</b>	<b>65.2</b>	<b>57.2</b>	<b>62.6</b>	<b>71.4</b>

**Table A1.** ViLex improves both image understanding and reconstruction capabilities of vision encoders by fine-tuning them using ViLex’s training approach. **Extending the fine-tuning of SigLIP with the ViLex approach from 150k to 600k steps results in improved overall model performance across evaluated benchmarks.** We use PaliGemma’s [6] framework for linear evaluation, replacing the vision encoder with either the fine-tuned SigLIP in ViLex or the official one, and freeze vision encoder and fine-tune the model on downstream tasks. We use the same hyper-parameters and model architecture for a fair comparison.

Below, you will see an input image along with two generated images, labeled as "Method A" and "Method B". Your task is to evaluate which image better meets specific criteria compared to the input image:

- **Semantic Alignment:** Which generated image more accurately captures the original content and semantic details, such as object categories? Note that it is less preferred if a model generates new instances or objects that were not in the input image or if it omits existing objects.
- **Style Alignment:** Which generated image better preserves the artistic style and visual aesthetics of the original?
- **Layout Alignment:** Which generated image maintains a composition and positioning of objects that aligns more closely with the input image?

For each criterion, please select the method (A or B) that you feel performs better. There are no right or wrong answers —please base your decision on your personal preference.

Input Image



Method A



Method B



Q1: Semantic Alignment

- Method A
- Method B

Q2: Style Alignment

- Method A
- Method B

Q3: Layout Alignment

- Method A
- Method B

**Figure A1.** The instructions and question format used for human study.

For GQA [30] (VQA on image scene graphs): learning rate (5e-6, 1e-5), and dropout (0.0, 0.02, 0.05). For Ref-COCO [33, 45, 83] (referring expression segmentation): label smoothing (0.1, 0.2), epochs (60, 100), and dropout (0, 0.05). For MSRVTT-Caps [78] (open-domain short video captioning): weight decay (0, 1e-6), dropout (0, 0.2), and epochs (20, 40).

## A2. Human Study

We conduct human studies to evaluate the quality of generated images using an image-to-image pipeline, focusing on three criteria: Semantic Alignment, Style Alignment, and

Layout Alignment. For Semantic Alignment, participants judge which generated image more accurately captures the original content and semantic details, such as object categories. Introducing new instances or omitting existing ones from the input image is considered less desirable. For Style Alignment, participants assess which generated image best retains the artistic style and visual aesthetics of the original. For Layout Alignment, participants evaluate which generated image maintains a composition and positioning of objects that closely matches the input image.

The results of this evaluation are reported in Table 2 of the main paper. Detailed instructions and the question for-



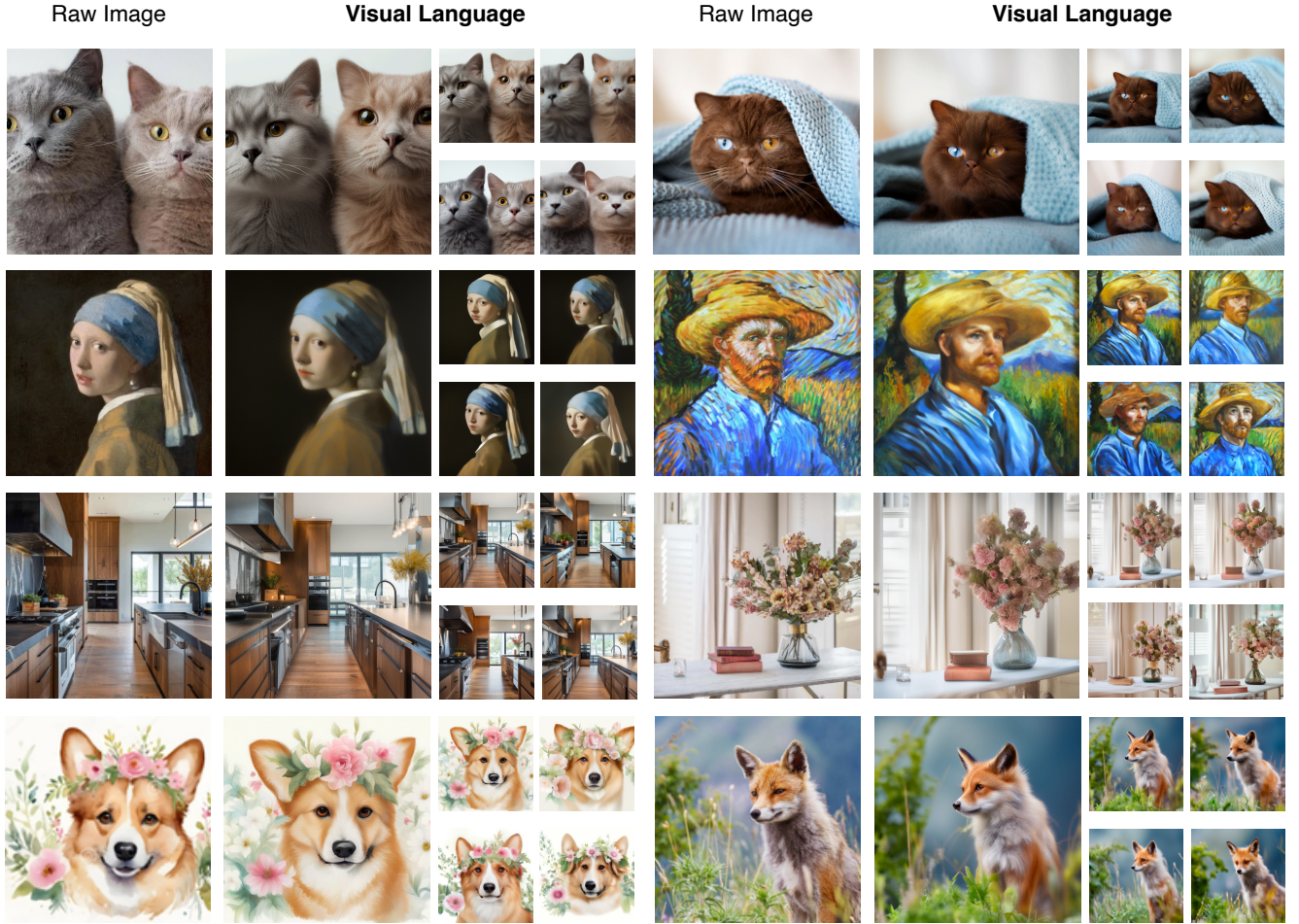


**Figure A2.** More demo results of generating a set of images (generated under different diffusion noises), which are highly semantically and visually similar to each other, by using ViLex tokens as “text” prompts for text-to-image diffusion models.

mat for the human study are shown in Figure A1.

### A3. Ablation Study

**Training Steps.** We observed that extending the fine-tuning steps of the vision encoder using our ViLex pipeline leads to improved performance across nearly all evaluated benchmarks, as shown in Table A1. Specifically, increasing the training steps from 150k to 300k yields significant gains. Further extending the training to 600k steps provides marginal improvements compared to the 300k-step results. The largest improvements are observed in datasets that demand stronger spatial understanding, such as the referring expression segmentation datasets RefCOCO+/g.

**Number of attention pooling layers.** Although increasing the number of attention pooling layers improves image reconstruction performance (as indicated by a lower FID score), it also introduces a trade-off with image understanding capabilities. As shown in Table A2, we found that using

5 attention pooling layers provides the optimal balance between image generation quality and developing an effective vision encoder for visual scene understanding.

#layers	FID	COCOCaps
2	2.62	140.7
5	2.58	141.5
8	2.52	141.0

**Table A2.** Ablation study on number of attention pooling layers.

**Vision encoders.** The ViLex approach effectively enhances various vision encoders for downstream visual scene understanding tasks. We initialize the vision encoder of ViLex with either the CoCa [82] pretrained ViT or the SigLIP [88] pretrained ViT-So400M. Similar to our experiments in previous sections, We observed consistent performance improvements for both image understanding tasks, such as COCOCaps [40], and video understanding tasks, such as

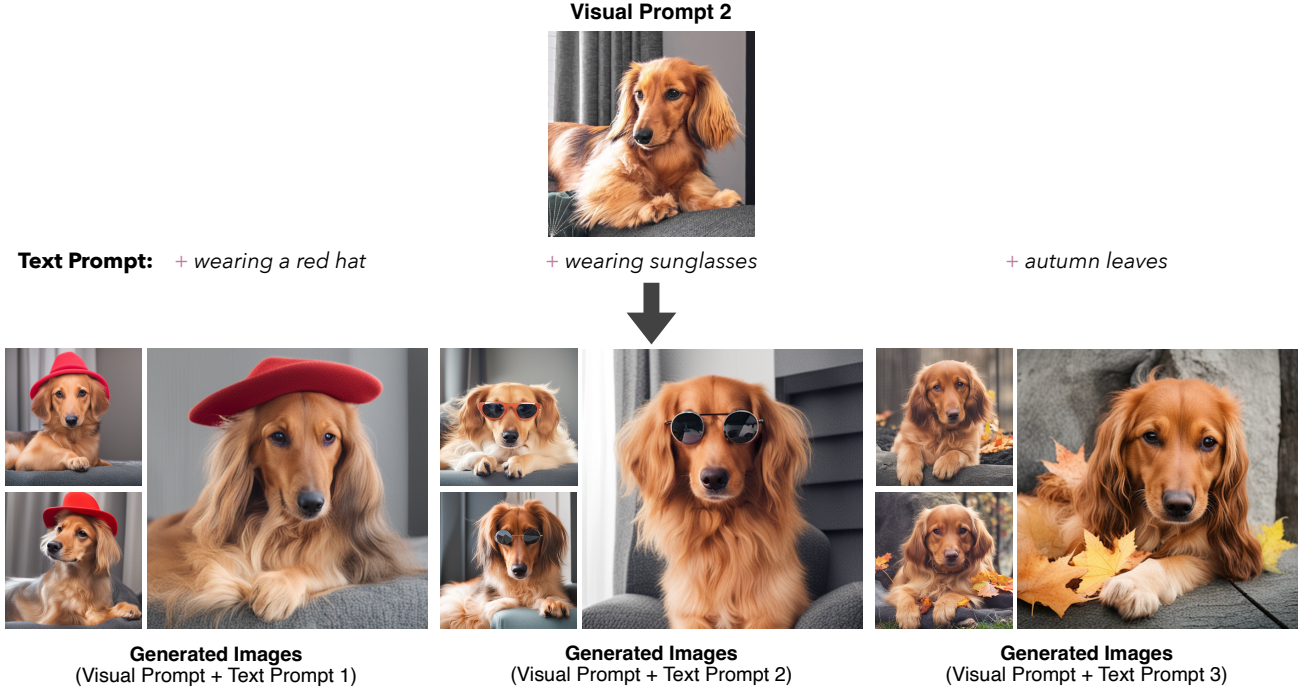


**Figure A3.** More demo results of zero-shot accessorization via prompting a frozen text-to-image generation model with our visual prompts (*i.e.*, ViLex tokens) and text prompts from natural language.

MSRVTT-Caps [78]. Compared to a roughly 2% improvement for SigLIP in terms of CIDEr score on COCOCaps, the gains for CoCa were even more substantial, reaching approximately 4%. The flexibility to consistently improve different pretrained models demonstrates ViLex’s generalizability across various types of vision encoders.

Datasets	CoCa	F.T. w/ ViLex	SigLIP	F.T. w/ ViLex
COCOCaps	131.6	<b>135.8</b>	139.7	<b>141.5</b>
MSRVTTCaps	56.1	<b>60.2</b>	69.4	<b>71.4</b>

**Table A3.** Fine-tuning vision encoders with the ViLex approach enhances image understanding performance across various pre-trained models, including CoCa [82] and SigLIP [88]. F.T. denotes fine-tuning the vision encoder, such as CoCa, during the ViLex model pretraining stage.

## A4. Demo Results

**Semantic-level image reconstruction.** In this section, we present additional demo results in Figure A2, showcasing a set of images generated with varying diffusion noises and different random seeds. These images demonstrate high semantic and visual consistency, leveraging ViLex tokens as “text” prompts for text-to-image diffusion models. However, as shown in the results, our model occasionally misses small objects in the scene. This limitation primarily stems from using a low-resolution text-to-image diffusion model

as the base during the ViLex model’s pretraining phase. We hypothesize that this issue could potentially be mitigated by employing a higher-resolution T2I model as the base model. **Prompting a frozen T2I model with both visual and textual prompts.** In the main paper, we have demonstrated that ViLex tokens can serve as a novel visual “language” for multimodal image generation. Unlike methods such as DreamBooth [58, 59] and textual inversion [18], which require: (1) learning specialized text tokens for specific instances, (2) gradient-based training for each individual image, and (3) the use of LORA adapters [29] to modify the model architecture, DreamBooth must be fine-tuned separately for each object (or each set of images corresponding to the same object). In contrast, ViLex enables several DreamBooth tasks like image re-contextualization, artistic rendition and accessorization, as illustrated in Figure A3, Figure 5 and Figure 6, by simply prompting a frozen T2I model with a combination of our visual prompts (*i.e.*, ViLex tokens) and natural language text prompts. This approach does not require changes to the architecture of a pretrained text-to-image generation model or any fine-tuning of the T2I model itself. All tasks are performed in a zero-shot and unsupervised manner.